Eur. Phys. J. C 33, 113–122 (2004)
Digital Object Identifier (DOI) 10.1140/epjc/s2003-01565-9

THE EUROPEAN PHYSICAL JOURNAL C

# Nucleus–nucleus interaction in the perturbative QCD

M.A. Braun[a]

Dep. High-Energy Physics, St. Petersburg University, 198504 St. Petersburg, Russia
North Carolina Central University, Durham, NC, USA

Received: 25 September 2003 / Revised version: 27 November 2003 /
Published online: 22 January 2004 – 

**Abstract.** The nucleus–nucleus interaction is studied in the framework of the perturbative QCD with $N_c \to \infty$ and a fixed coupling constant. The pomeron tree diagrams are summed by an effective field theory. The classical field equations are solved by an iteration procedure, which is found to be convergent in a restricted domain of not too high energies and atomic numbers. The found gluon distributions do not scale, have their maxima close to $2\,\mathrm{GeV}/c$ independent of rapidity and fall towards the central rapidity region. The cross-sections slowly grow with energy due to the contribution from peripheral collisions, where evolution remains linear. Simple variational estimates at higher rapidities confirm this tendency.

## 1 Introduction

As discussed in [1] in the perturbative QCD with a large number of colors $N_c$ and a fixed coupling constant high-energy nucleus–nucleus interaction is described by the exchange of an arbitrary number of BFKL pomerons, which interact between themselves via the three-pomeron coupling. Corrections due to interactions not reducible to pomeron exchange but rather to gluonic exchange are of the order $1/N_c^2$. The resulting pomeronic diagrams can be classified according to the number of pomeronic loops. Each pomeronic loop gives an additional factor $1/N_c^2$. So in the high-color limit only tree diagrams survive. In the case of the scattering on the nucleus of a very small probe (e.g a highly virtual photon) this leaves only pomeronic fan diagrams, which can easily be summed to lead to the non-linear BFKL evolution equation [2–4]. This equation, although not soluble analytically, can be comparatively easily solved by numerical methods (e.g. [4–6]).

For nucleus–nucleus scattering the situation complicates enormously. The basic complication comes from the fact that now the pomerons not only split into two but also merge from two to one. The tree diagrams now do not reduce to fans but involve other structures, as shown in Fig. 1. Still, using the methods of effective non-local field theory, one can sum all these diagrams, reducing the problem to the solution of a pair of non-linear field equations in the rapidity-transverse momentum space [1]. Unfortunately, contrary to the non-linear BFKL equation, these are not evolution equations but rather correspond to a system of full-fledged non-linear integral equations, which are very difficult to solve.

In this paper we make a first attempt at a solution of these equations and try to gain some insight into the physical picture of the nucleus–nucleus interaction in this approach. We use two different methods of solution. First we try to find the solution by iterative methods starting from the fan diagrams only. Unfortunately our results show that this method is convergent in a very restricted region of not too high rapidities and not too large nuclei. Beyond this region the iterations do not converge, indicating some sort of qualitative change in the form of the solution (a phase transition?). In relation to this it is worth remembering that the primitive Glauber approximation formula for the nucleus–nucleus scattering in the tree approximation shows a similar singularity as the nuclei become heavy enough (at $A = 64$ for nuclei with a constant profile function within their transverse areas) [7]. To move beyond the mentioned limits we tried to use a direct variational method to find the stationary point of the effective action, choosing the simplest form of the trial fields. Comparison with the exact solution where it can be found by iterations shows that the precision of our variational results is not high (of the order $\sim 30\%$). Still it gives a possibility to see the qualitative behavior of the solutions at very high rapidities.

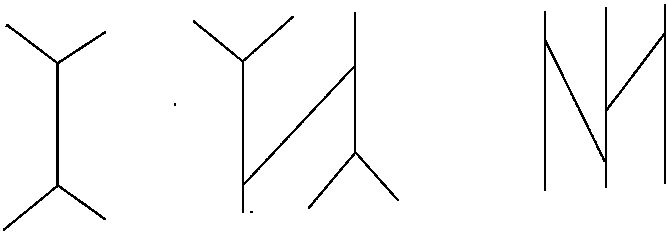

**Fig. 1.** Some pomeron tree diagrams summed by our effective field theory

Our results show that in the nucleus–nucleus collisions the rise of the effective number of gluons becomes still more

[a] e-mail: mijail@fpaxp1.usc.es

suppressed than in the non-linear BFKL equation case. In fact the variational estimates indicate that it may even go down with the growth of the rapidity. However this is not clearly reflected in the final nucleus–nucleus cross-sections, which continue to slowly rise due to the contribution from the peripheral parts of the nuclei, where, due to the small nuclear density, the evolution remains practically linear.

In general, the effect of the pomeron interaction on the nuclear cross-section is not very impressive. This is a consequence of the fact that the nucleus–nucleus amplitude gets automatically unitarized due to cancellations between contributions of different disconnected parts. A much greater change can be seen in the contribution of each such part (the eikonal function), which at high rapidity becomes many orders of magnitude smaller than in the pure linear BFKL evolution case.

This paper is organized as follows. In Sect. 2 we recall our basic formalism to treat the nucleus–nucleus collisions in the perturbative QCD approach, which reduces the problem to searching a stationary point for the action of a certain non-linear and non-local field theory. In Sect. 3 we outline our methods to find this stationary and to solve the corresponding variational field equations. Section 4 presents our numerical results, which are discussed in Sect. 5.

## 2 $AB$-cross-sections and effective field theory

At fixed overall impact parameter $b$ and (high) rapidity $Y$ the nucleus-$A$–nucleus-$B$ total cross-section is given by

$$\sigma(Y,b) = 2\left(1 - \mathrm{e}^{-T(Y,b)}\right). \tag{1}$$

Here the eikonal function $T$ is a contribution from the connected part and is an integral over two impact parameters $b_A$ and $b_B$ of the collision point relative to the centers of the nuclei $A$ and $B$:

$$T(Y,b) = \int \mathrm{d}^2 b_A \mathrm{d}^2 b_B \delta^2(b - b_A + b_B) T(Y, b_A, b_B). \tag{2}$$

In perturbative QCD, in the large $N_c$ limit, the eikonal function is given by a sum of all connected tree diagrams constructed of BFKL pomerons, which interact between themselves via the triple pomeron vertex (with a minus sign). It can be shown that this sum is generated by an effective field theory of two fields $\phi(y,q)$ and $\phi^\dagger(y,q)$ depending on the rapidity $y$ and transverse momentum $q$ with an appropriately chosen action $S$ [1]. The action consists of a free part $S_0$, an interaction part $S_\mathrm{I}$ and an external part $S_\mathrm{E}$. The free part is given by

$$S_0 = 2\left\langle \phi^\dagger \left| K\left(\frac{\partial}{\partial y} + H\right)\right| \phi \right\rangle, \tag{3}$$

where $H$ is the forward BFKL Hamiltonian for the so-called semi-amputated amplitudes [8] and $K$ is a differential operator in $q$ commuting with $H$:

$$K = \nabla_q^2 q^4 \nabla_q^2. \tag{4}$$

The symbol $\langle \ldots \rangle$ means integrating over $y$ and $q$ with weight $1/(2\pi)^2$ The action $S_0$ generates propagators which are BFKL Green functions with operators $K^{-1}$ attached at their ends. The interaction part of the action describes splitting and merging of pomerons:

$$S_\mathrm{I} = \frac{4\alpha_\mathrm{s}^2 N_c}{\pi} \left\langle \left( {\phi^\dagger}^2 K\phi + \phi^2 K \phi^\dagger \right) \right\rangle. \tag{5}$$

The coefficient in this term depends on the normalization of the fields. Finally the external action is

$$S_\mathrm{E} = -\left\langle \left( w_A \phi + w_B \phi^\dagger \right) \right\rangle, \tag{6}$$

where $w_{A,B}$ describe the interaction of the pomerons with the projectile and target. If the color distribution in the target is given by

$$\rho_A(r) = g^2 A T_A(b_A) \rho(r), \tag{7}$$

where $\rho(r)$ is the color distribution in the nucleon and $T_A$ is the target nucleus profile function, then

$$w_A(y,q) = \delta(y) \int \mathrm{d}^2 r r^2 \rho_A(r) \equiv \delta(y) \hat{w}_A(q), \tag{8}$$

the $\delta$ function indicating that the target is taken to be at zero rapidity. The function $w_B(y,q)$ is given by a similar formula with $\delta(y)$ substituted by $\delta(y-Y)$ where $Y$ is the rapidity of the projectile.

The classical equations of motion which follow, multiplied by $(1/2)K^{-1}$ from the left, are

$$\left(\frac{\partial}{\partial y} + H\right)\phi + \frac{2\alpha_\mathrm{s}^2 N_c}{\pi}\left(\phi^2 + 2K^{-1}\phi^\dagger K \phi\right) = \frac{1}{2} K^{-1} w_A \tag{9}$$

and

$$\left(-\frac{\partial}{\partial y} + H\right)\phi^\dagger + \frac{2\alpha_\mathrm{s}^2 N_c}{\pi}\left({\phi^\dagger}^2 + 2K^{-1}\phi K \phi^\dagger\right) = \frac{1}{2} K^{-1} w_B. \tag{10}$$

From the $\delta$-like dependence on $y$ of the external sources it follows that the equations can be taken to be homogeneous in the interval $0 < y < Y$, the action of the external sources being substituted for by the boundary conditions

$$\phi(0,q) = \frac{1}{2} K^{-1} \hat{w}_A(q), \qquad \phi^\dagger(Y,q) = \frac{1}{2} K^{-1} \hat{w}_B(q). \tag{11}$$

The eikonal function $T(Y, b_A, b_B)$ is just the action $S$ calculated with the solutions of (9) and (10), $\phi_\mathrm{cl}$ and $\phi_\mathrm{cl}^\dagger$:

$$T(Y, b_A, b_B) = -S\{\phi_\mathrm{cl}, \phi_\mathrm{cl}^\dagger\}. \tag{12}$$

Using the equation of motions one can somewhat simplify the expression for $S$. Indeed multiplying the first equation

by $2K\phi^\dagger$, the second one by $2K\phi$, integrating both over $y$ and $q$ and summing the results, one obtains the relation

$$2S_0 + 3S_\mathrm{I} + S_\mathrm{E} = 0, \tag{13}$$

which is valid for the classical action, that is, one calculated with the solutions of (9) and (10). Using this relation we can exclude, say, $S_0$ from (12) to find

$$T(Y, b_A, b_B) = \frac{1}{2}\left(S_\mathrm{I}\left\{\phi_\mathrm{cl}, \phi^\dagger_\mathrm{cl}\right\} - S_\mathrm{E}\left\{\phi_\mathrm{cl}, \phi^\dagger_\mathrm{cl}\right\}\right). \tag{14}$$

The dependence on $b_A$ and $b_B$ comes from the boundary conditions (11).

## 3 Methods of solution

### 3.1 Final formulas for calculation

To solve (9) and (10) we first rescale the rapidity and fields to pass to variables known from studying fan diagrams [3,4]:

$$y \to y/\bar\alpha, \quad H \to \bar\alpha H, \quad \phi \to \frac{1}{2\alpha_\mathrm{s}^2}\phi, \quad \phi^\dagger \to \frac{1}{2\alpha_\mathrm{s}^2}\phi^\dagger, \tag{15}$$

where, as is standard, $\bar\alpha = \alpha_\mathrm{s} N_c/\pi$. In these variables, for $0 < y < Y$, the equations of motion have the same form (9) and (10) without the coefficient before the non-linear terms and with zero right-hand side. All parts of the action acquire a common coefficient $1/(2\alpha_\mathrm{s}^2)$:

$$S_0 = \frac{1}{2\alpha_\mathrm{s}^2}\left\langle \phi^\dagger K\left(\frac{\partial}{\partial y} + H\right)\phi\right\rangle, \tag{16}$$

$$S_\mathrm{I} = \frac{1}{2\alpha_\mathrm{s}^2}\left\langle \left(\phi^{\dagger 2} K\phi + \phi^2 K\phi^\dagger\right)\right\rangle \tag{17}$$

and

$$S_\mathrm{E} = -\frac{1}{2\alpha_\mathrm{s}^2}\left\langle \phi^\dagger K\phi\left(\delta(y) + \delta(y-Y)\right)\right\rangle, \tag{18}$$

where we expressed the external sources via the boundary values of $\phi$ and $\phi^\dagger$. Note that the expression for $S_0$ assumes integration over all values of $y$, so that the derivative in $y$ generates $\delta$-like terms which partially cancel with the external part of the action. If one symmetrizes $S_0$ in $\phi$ and $\phi^\dagger$, then these terms cancel exactly one half of $S_\mathrm{E}$. This implies that taking in $S_0$ the integration over $y$ in the interval $0 < y < Y$ one has to take the total action as

$$S = S_0 + S_\mathrm{I} + \frac{1}{2}S_\mathrm{E}. \tag{19}$$

The operator $K^{-1}$ appearing before the second non-linear term in (9) and (10) can be represented as an integral operator in the transverse momentum space with a kernel [1]

$$K^{-1}(q_1, q_2) = \frac{\pi}{2}\frac{1}{q_>^2}\left(\ln\frac{q_>}{q_<} + 1\right), \tag{20}$$

where $q_{>(<)} = \max(\min)\{q_1, q_2\}$. The operator $K$ contains the 4th derivative in $q$. To simplify it we present it as a product

$$K = L^\dagger L, \qquad L = q^2\nabla_q^2. \tag{21}$$

In logarithmic variables $L$ reduces to the 2nd derivative. If

$$q = q_0 \mathrm{e}^{\beta t}, \tag{22}$$

then

$$L = \frac{1}{\beta^2}\frac{\partial^2}{\partial t^2}. \tag{23}$$

Using this and integrating by part to exclude higher derivatives we can express the complicated 2nd non-linear term in the equations via the functions $\phi$ and $\phi^\dagger$ and their first and second derivatives in $t$. Denoting

$$\frac{\partial\phi}{\partial t} = \phi_1, \quad \frac{\partial^2\phi}{\partial t^2} = \phi_2 \tag{24}$$

and similarly for $\phi^\dagger$, we find

$$\begin{aligned} &2K^{-1}\phi^\dagger K\phi \\ &= \frac{1}{2\beta^3}\left\{\int_{-\infty}^{t} \mathrm{d}t_1 \mathrm{e}^{-2z}\phi_2\left((z+1)\phi_2^\dagger - 2\beta\phi_1^\dagger\right)\right. \\ &\left. + \int_t^\infty \mathrm{d}t_1\phi_2\left((1-z)\phi_2^\dagger + 2\beta(2z-1)\phi_1^\dagger - 4\beta^2 z\phi^\dagger\right)\right\}, \end{aligned} \tag{25}$$

where $z = \beta(t - t_1)$. The conjugated term has the same form with $\phi \leftrightarrow \phi^\dagger$.

Calculating the action one can split $K$ into a pair of operators $L$ acting on factors depending on $\phi$ and $\phi^\dagger$. In this way one obtains

$$S_0 = \frac{1}{2\alpha_\mathrm{s}^2\beta^4}\left\langle \phi_2^\dagger\left(\frac{\partial}{\partial y} + H\right)\phi_2\right\rangle \tag{26}$$

(symmetrized in $\phi$ and $\phi^\dagger$),

$$S_\mathrm{I} = \frac{1}{2\alpha_\mathrm{s}^2\beta^4}\left\langle 2\phi_2(\phi_2^\dagger\phi + \phi_1^2) + \mathrm{h.c.}\right\rangle, \tag{27}$$

$$S_\mathrm{E} = -\frac{1}{2\alpha_\mathrm{s}^2\beta^4}\left\langle \phi_2^\dagger\phi_2\left(\delta(y) + \delta(y-Y)\right)\right\rangle. \tag{28}$$

### 3.2 Boundary conditions

To fix our boundary conditions we use our experience with the non-linear BFKL equation to study the nuclear structure functions [4,6]. The adequate initial values for $\phi(y, q)$ were taken there from the Golec-Biernat–Wuesthoff distribution, fitted to the proton data at comparatively low values of $x$ [9], which was duly eikonalized for a nucleus target. In fact, eikonalization implies including terms of higher orders in $1/N_c^2$, outside the precision of the approach. Also it is not clear how to generalize the eikonalization procedure to the nucleus–nucleus case. For both of these reasons our

first choice (I) for the initial values is the non-eikonalized Golec-Biernat–Wuesthoff distribution for the nucleus:

$$\phi(0,q) = -\frac{1}{2} a \,\mathrm{Ei}\left(-\frac{q^2}{0.21814}\right). \tag{29}$$

Here $a$ carries information about the nucleus and impact parameter

$$a = \sigma_0 T_A(b_A), \tag{30}$$

$\sigma_0 = 20.8\,\mathrm{mb}$ and $q$ is in GeV/$c$. The value of $\phi^\dagger(Y,q)$ was taken in the same form with $T_A(b_A) \to T_B(b_B)$. To study a possible influence of the form of the initial distribution in $q$ we also used the alternative choice (II) with the same infrared behavior and point where the gluon distribution is peaked, but a much slower fall of the distribution at large $q$,

$$\phi(0,q) = -\frac{1}{2} a \ln\left(1 + \frac{0.21814}{q^2}\right). \tag{31}$$

### 3.3 Iterative solution

Our first method to find the stationary point of the action has been to solve the classical equations of motion iteratively. We have chosen the sum of pure fan diagrams as a starting function for the iterations. In practice this means that we first solve the equations with the non-linear term mixing $\phi$ and $\phi^\dagger$ put to zero. These solutions serve as input for the iterations $\phi^{(o)}$ and $\phi^{\dagger\,(0)}$. Then we find the next iterations from the equations

$$\left(\frac{\partial}{\partial y} + H\right)\phi^{(n+1)} + {\phi^{(n+1)}}^2 + 2K^{-1}\phi^{\dagger(n)} K \phi^{(n)} = 0 \tag{32}$$

and

$$\left(-\frac{\partial}{\partial y} + H\right)\phi^{\dagger(n+1)} + {\phi^{\dagger(n+1)}}^2 + 2K^{-1}\phi^{(n)} K \phi^{\dagger(n)} = 0. \tag{33}$$

For each iteration we only have to evolve the initial function from $y = 0$ to $y = Y$, rather than solve the equivalent pair of two dimensional non-linear integral equations, which considerably diminishes computer time.

Unfortunately our calculations show that this method works only for rather small values of the participant atomic numbers and rapidity $Y$. Obviously the maximal value of the factor $a$ entering (29) or (30) is achieved at $b = 0$ and for $\max\{A, B\}$. With the Woods–Saxon nuclear density for Pb–Pb, Cu–Cu, Al–Al, O–O and C–C collisions this $\max\{a\}$ is found to be equal to 2.20, 1.53,1.11, 0.88 and 0.83 respectively. Our calculations show that for $a \le 2.2$ the described iteration procedure is convergent only up to $Y = 1.1$ for choice I of the initial distribution and up to $Y = 1.8$. for choice II. For lighter nuclei, taking $a \le 1.0$ we find that iterations converge up to $y = 1.3$ for choice I and up to $Y = 2$ for choice II. The physical values of these rapidities depend on the chosen value of $\bar\alpha$. With $\bar\alpha = 0.2$ the above numbers are to be multiplied by a factor 5, but still remain rather low: for, say, O–O collisions the iterations allow one to move only up to rapidities of the order 10, that is, CM energies of the order of 150 GeV and for Pb–Pb collisions the upper limit for the CM energy lowers to $\sim 90\,\mathrm{GeV}$.

### 3.4 Variational solution

A clear alternative is obviously to try to directly find the stationary point of the action choosing some trial fields $\phi(y,q)$ and $\phi^\dagger(y,q)$ which satisfy the boundary conditions. The difficulty of this approach is related to the fact that the action can have more than one stationary point. In our first attempt we have chosen the simplest form for the trial fields with $y$ and $q$ dependence factorized. Moreover, for the $y$ dependence we chose a simple exponential one, with a variable slope $\Delta$, so that our trial fields have the form

$$\phi(y,q) = \mathrm{e}^{\Delta y}\phi(0,q), \quad \phi^\dagger(y,q) = \mathrm{e}^{\Delta(Y-y)}\phi^\dagger(Y,q) \tag{34}$$

The boundary functions $\phi(0,q)$ and $\phi^\dagger(Y,q)$ were taken according to (29) and (30) for variants I and II. The only variational parameter, $\Delta$, was chosen to give the minimal value for the action $S$. Note that, with the fields having a simple analytic form, the necessary derivative functions entering (26)–(28) are easily found, so that calculating the action reduces to just doing two independent integrations, over $y$ and $q$. With these trial fields the solution for $\Delta$ always exists for any values of $Y$ and parameter $a$ in (29)–(30), and moreover it corresponds to the minimum of the action. The quality of this approximation can be checked at $y$ and $a$ where the exact solution can be found perturbatively. At $Y = 1$ and $a = 1$ the exact values of the action $S$ (without factor $1/(2\alpha_s^2)$) are $-0.0120$ and $-0.0370$ for variants I and II, respectively. The variational values obtained with (34) for these two variants are $-0.0100$ and $-0.0262$. As one observes the precision is not very high (especially for variant II). Still we hope that the variational approach might give some indication about the behavior of the cross-section and eikonal functions at large values of $Y$ at which we cannot obtain the exact solution.

## 4 Numerical results

We first report on the iterational solution of the field equations (32) and (33), which, as mentioned, is convergent at not too high values of $Y$, $A$ and $B$. We chose to study O–O scattering ($A = B = 16$) using choice II of the initial functions, which allowed us to obtain the solution up to $Y = 2$. Presenting our results we first consider the gluonic density, which can be related to the functions $L\phi(y,q) = h(y,q)$ and $L\phi^\dagger(y,q) = h^\dagger(y,q)$. Indeed, as follows from the study of the non-linear BFKL equation, the gluon density of a single heavy nucleus is given by [4]

$$\frac{\mathrm{d}xG(x,q)}{\mathrm{d}^2b\mathrm{d}^2q} = \frac{N_c}{2\pi^2\alpha_s} h(y,q), \quad y = \bar\alpha \ln\frac{1}{x}. \tag{35}$$

Note that this density in fact describes the interaction with the nucleus of a quark–antiquark pair and so can

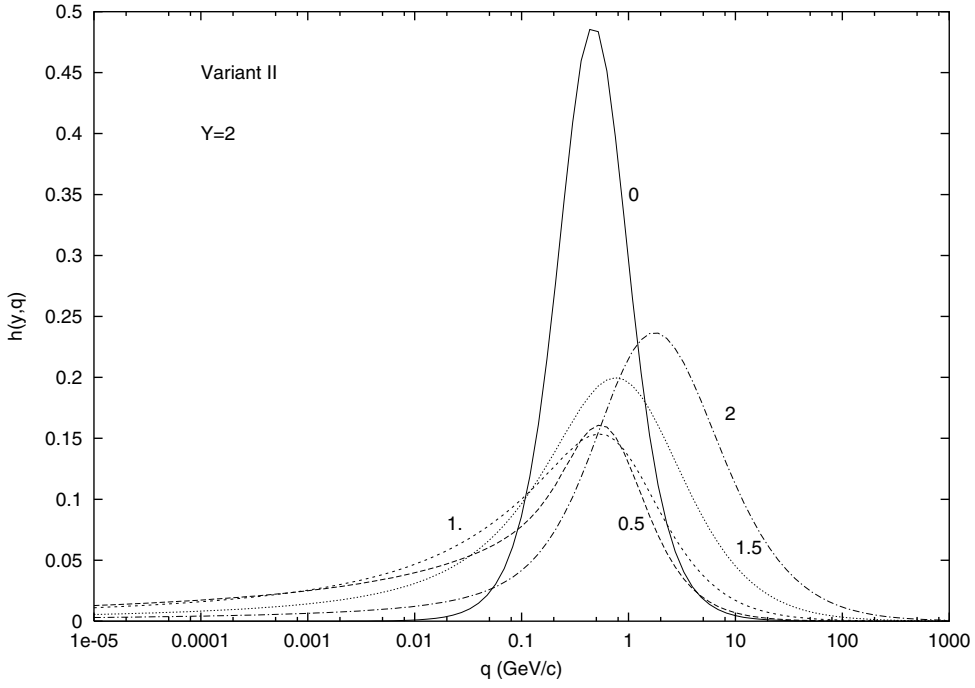


**Fig. 2.** The gluon distribution corresponding to the field $\phi(y,q)$ with initial function II. Numbers show rapidities $y = 0$, 0.5, 1, 1.5 and 2

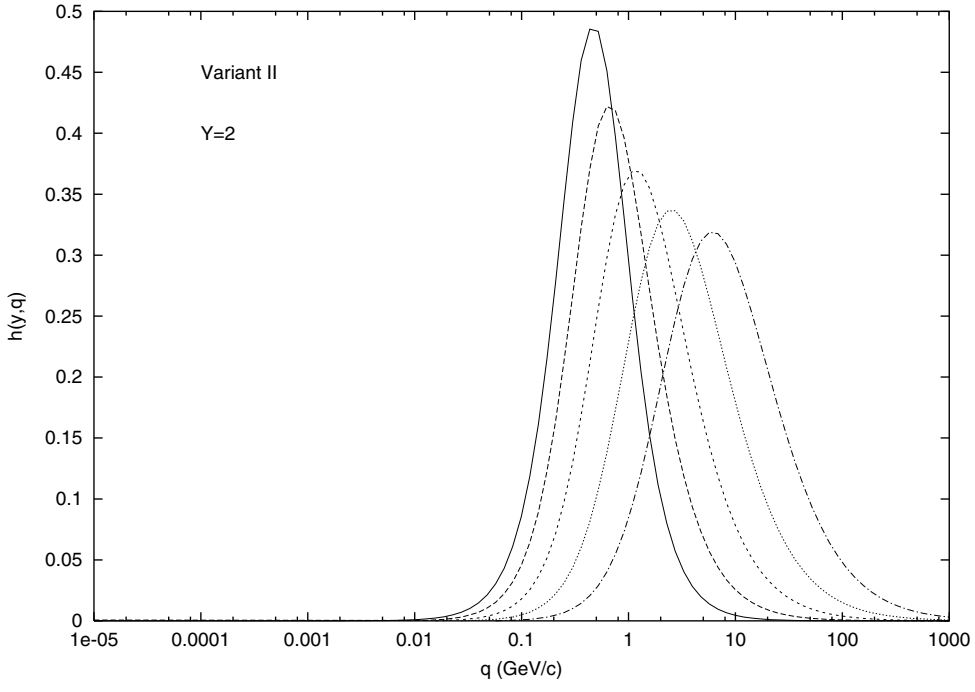


**Fig. 3.** Same as Fig. 2 for the field evolving according to the non-linear BFKL equation (only fan diagrams). Curves from left to right correspond to $y = 0$, 0.5, 1, 1.5 and 2

be measured in $\gamma^*$–nucleus collisions. However, it does not correspond directly to the spectrum of gluon jets produced in collisions with the nucleus, which is rather given by the convolution of (35) with the gluon density in a single BFKL pomeron [10]. We conjecture that the analogous gluon density in the nucleus–nucleus collision at rapidity $y$ will be given by a similar formula with contributions from both nuclei. For central collisions then

$$\frac{\mathrm{d}xG(x,q)}{\mathrm{d}^2b\mathrm{d}^2q} = \frac{N_c}{2\pi^2\alpha_\mathrm{s}}\left(h(y,q)+h^\dagger(y,q)\right). \qquad (36)$$

Note that in the considered symmetric case $\phi^\dagger(y,q) = \phi(Y-y,q)$ and so $h^\dagger(y,q) = h(Y-y,q)$.

As for a single nucleus, the density (36) describes the interaction of a quark–antiquark loop with two nuclei simultaneously. So, to measure it one has to introduce the loop into the interaction area of the two nuclei, which is obviously hardly realizable from the practical point of view. Unlike the single nucleus case, the density (36) seems to have no relation to the inclusive jet production spectrum (at least in the central region). Due to AGK cancellations the latter is given by a convolution of only fan

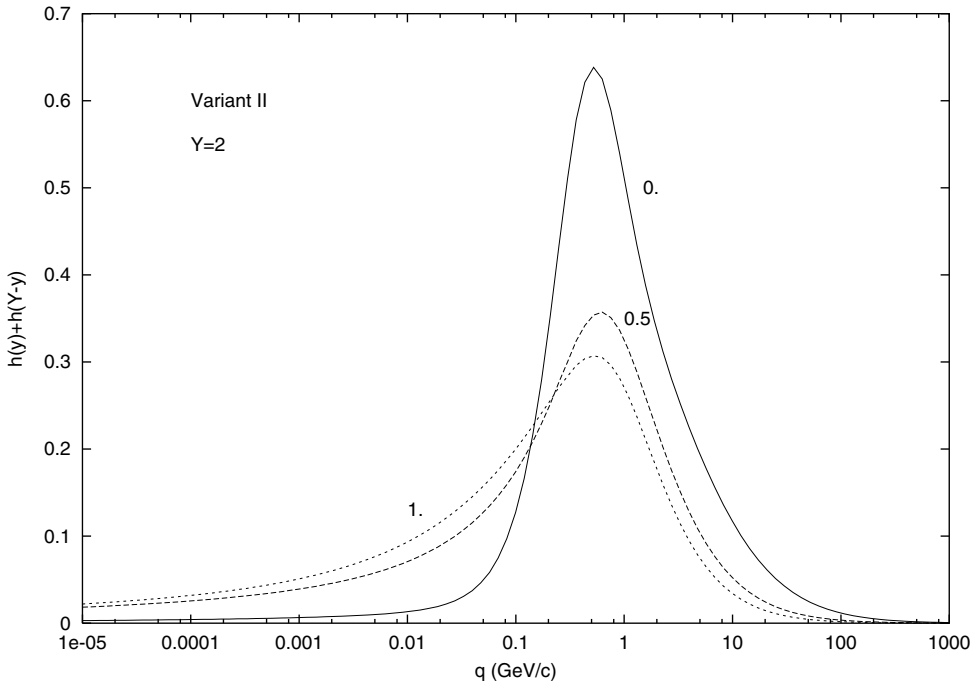


**Fig. 4.** The total gluon density in O–O collisions. Numbers show rapidity distances from the target or projectile: $y = 0$, 0.5 and 1

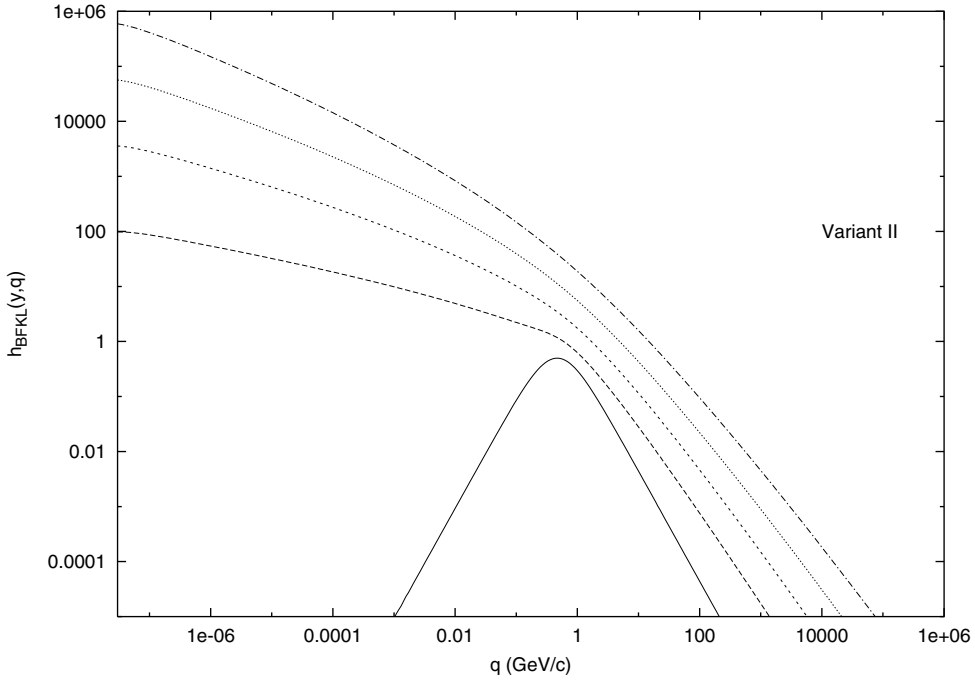


**Fig. 5.** Same as Fig. 2 for the field evolving according to the linear BFKL equation. Curves from bottom to top correspond to rapidities $y = 0$, 0.5, 1, 1.5 and 2

diagrams connected to both nuclei [1]. So the density (36) is a rather theoretical construction, which describes the proper gluon field of the two colliding nuclei just as for a single nucleus (35) describes its proper gluon field. The study of (36) allows one to see the change of this field due to the nuclear interaction.

In Fig. 2 we present our solution for $h(y, q)$ at $Y = 2$, $b_A = b_B = 0$ at different stages of the evolution: $y = 0$, 0.5, 1.0, 1.5 and 2. For comparison we show in Fig. 3 the same function which is found from the non-linear evolution equation for a single nucleus (only fan diagrams). The difference between Figs. 2 and 3 comes from the influence of another nucleus on the evolution process. As one can conclude, this influence is quite strong. Whereas the fan-diagram density steadily shifts towards higher momenta more or less preserving its shape, the density for the nucleus–nucleus collision practically does not move until $y = 1$, its peak dramatically falling and its low momentum tail visibly growing. Only as late as at $y = 1.5$ one notices some slow shift towards higher momenta, which becomes more pronounced at $y = 2$. Still at $y = 2$ its peak lies at $q = Q_s = 2\,\mathrm{GeV}/c$ ("saturation momentum"), whereas

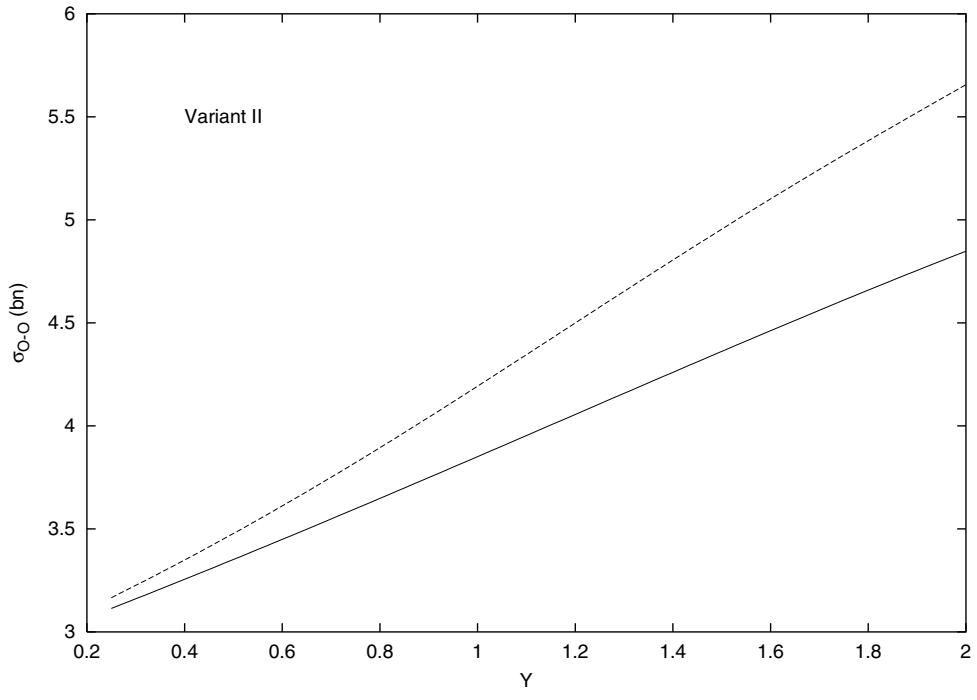


**Fig. 6.** The total cross-section for O–O collisions with initial conditions II (lower curve). The upper curve corresponds to a single BFKL exchange

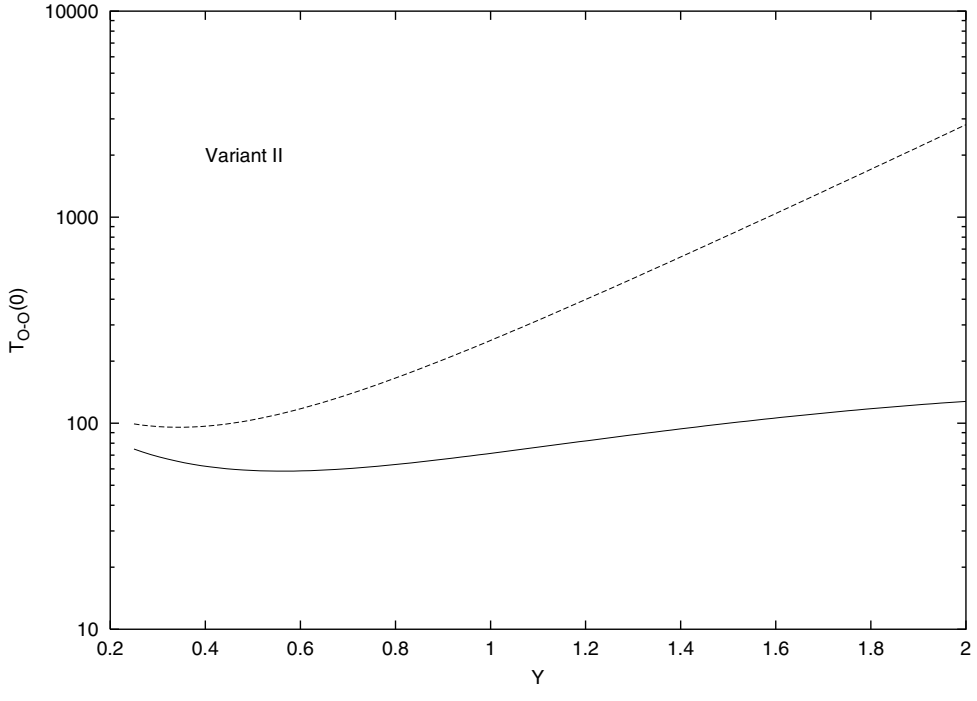


**Fig. 7.** The eikonal function at $b = 0$ for O–O collisions with initial conditions II (lower curve). The upper curve corresponds to a single BFKL exchange

for a single nucleus it is found at $Q_s = 8\,\mathrm{GeV}/c$. In Fig. 4 we illustrate the total gluon density in O–O collisions at $y = 2$ given by the sum $h(y,q) + h(Y-q)$ up to a factor depending on the coupling constant value. This density has its peak at the point close to $1\,\mathrm{GeV}/c$, practically independent of the rapidity. The height of the peak is falling towards the central region. Some diffusion towards small momenta is observed. It can however hardly be compared to the diffusion for the pure BFKL evolution illustrated in Fig. 5 for the same initial function and same region of $y$.

A clear physical observable is of course the total nucleus--nucleus cross-section obtained by the integration of (1) over all impact parameters. We show this for O–O scattering at $Y \leq 2$ in Fig. 6. To compare we present also the cross-sections corresponding to a single BFKL exchange. The latter are naturally larger but the difference is not at all dramatic, reaching some 18% at the maximal rapidity $Y = 2$. This is understandable, having in mind that (1) actually automatically unitarizes the amplitude and leads to very similar results even for very different eikonal func-

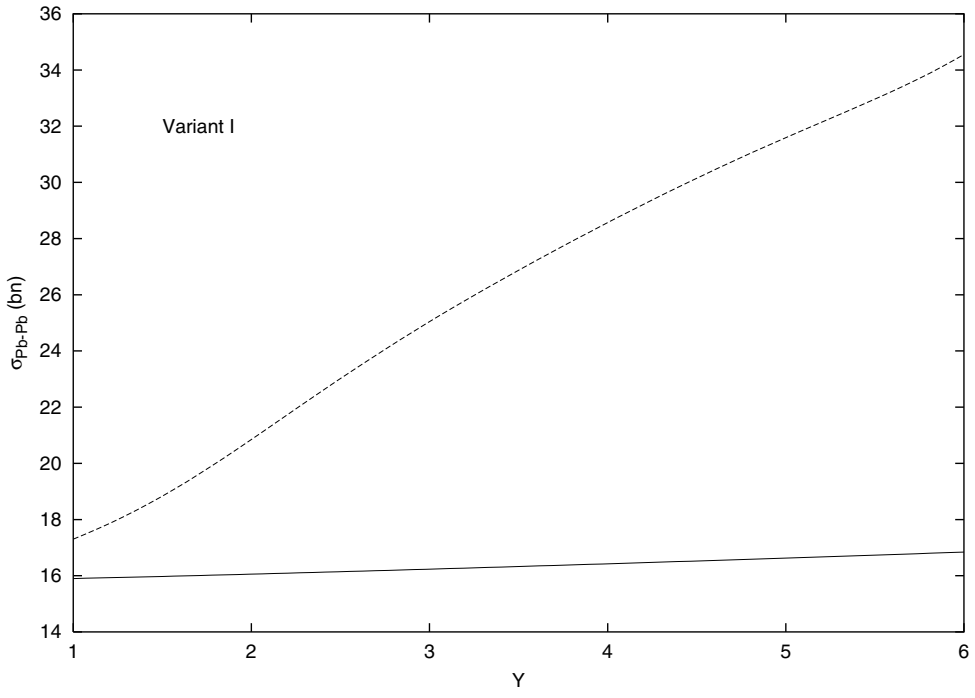


**Fig. 8.** Variational estimates for the total cross-sections for Pb–Pb collisions at high rapidities with initial conditions I (lower curve). The upper curve corresponds to a single BFKL exchange

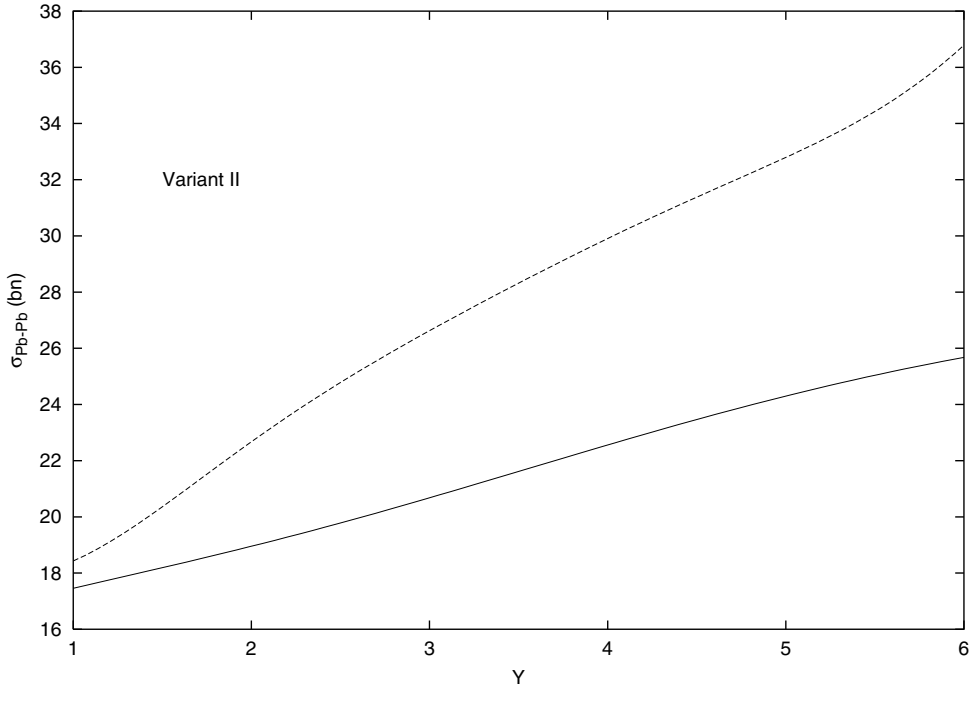


**Fig. 9.** Same as in Fig. 8 for initial conditions II

tions provided they are large. This can be clearly seen from the comparison of the eikonal functions at $b = 0$ in Fig. 7. At $Y = 2$ the pomeron interaction in the nucleus–nucleus collisions reduces it by an order of magnitude, although it still remains large, $\sim 200$. Some spreading of the gluon distribution into the low momenta domain visible in Fig. 4 in the central rapidity region makes one think that the results may be rather sensitive to the infrared region and so strongly dependent on the infrared cutoff. Such a dependence indeed exists but is not so strong. With the infrared cutoff at $k_{\min} = 0.3\,\mathrm{GeV}$ we obtain at $Y = 2$ $\sigma_{\mathrm{O-O}} = 4.18\,\mathrm{bn}$ and $T_{\mathrm{O-O}}(0) = 179$, whereas without cutoff we have $\sigma_{\mathrm{O-O}} = 5.36\,\mathrm{bn}$ and $T_{\mathrm{O-O}}(0) = 208$. As one observes the cross-section as a result is more sensitive to the infrared cutoff, which is a result of peripheral collisions, where the evolution follows the linear BFKL equation.

Our variational results for both variants of the choice of the initial functions are presented in Figs. 8–11. Since in this approximation we are not restricted to small values of $A$ and $B$, we show our results for Pb–Pb collisions

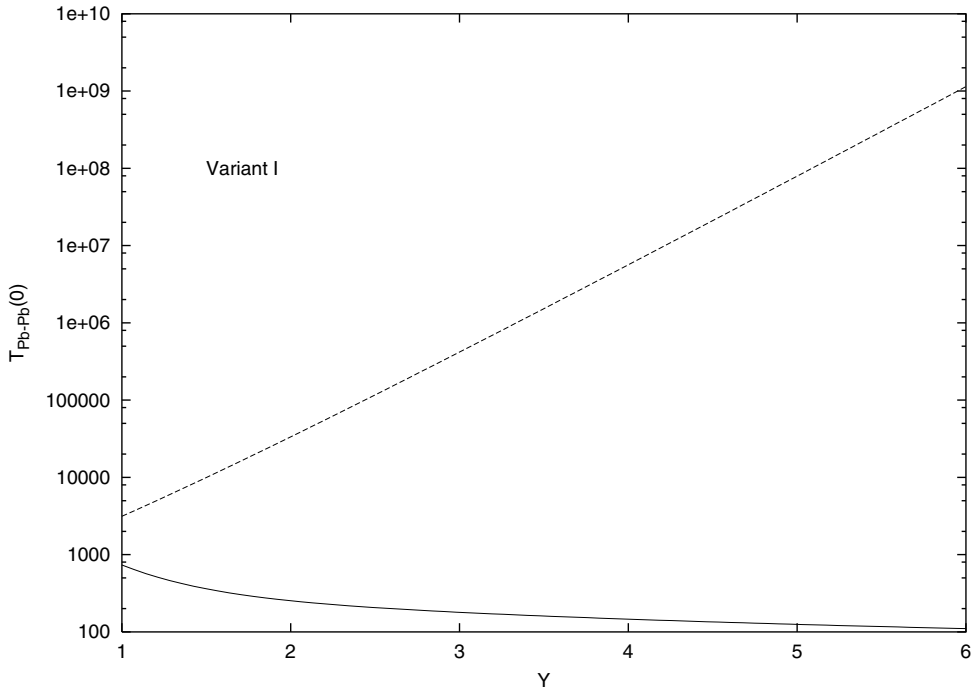


**Fig. 10.** Variational estimates for the eikonal function at $b = 0$ for Pb–Pb collisions at high rapidities with initial conditions I (lower curve). The upper curve corresponds to a single BFKL exchange

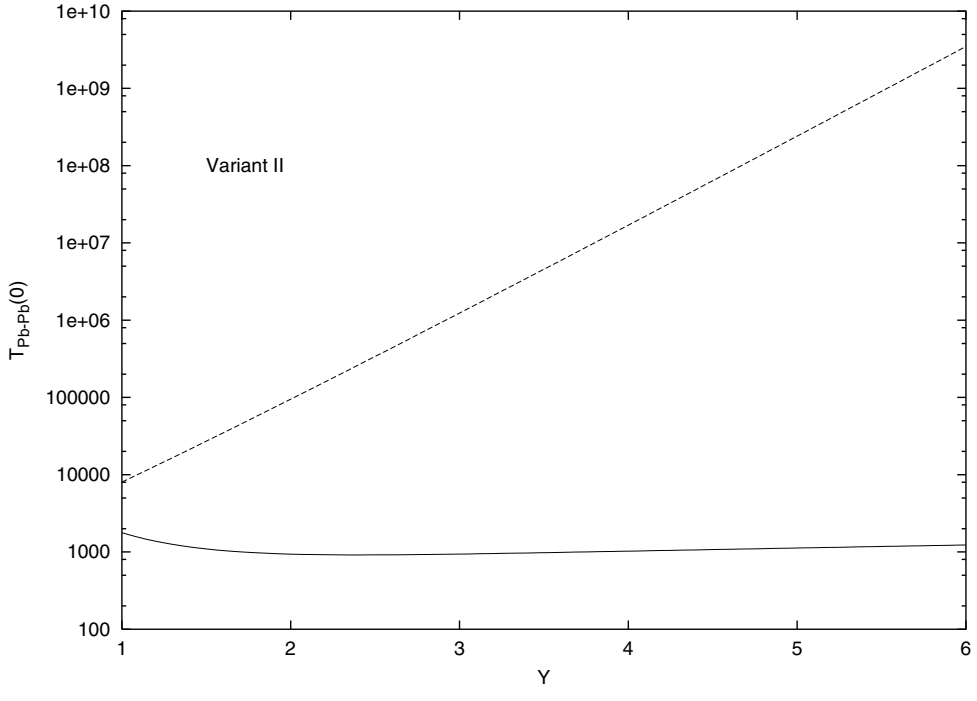


**Fig. 11.** Same as in Fig. 10 for initial conditions II

($A = B = 207$) In Figs. 8 and 9 we show the total cross-sections for variants I and II of the initial fields. They are again compared to the cross-sections corresponding to the single BFKL exchange. All the cross-sections steadily rise with $Y$. However, this rise seems to be very weak for choice I of the initial function. The single BFKL exchange naturally leads to larger cross-sections and the ratio of these to the cross-sections with pomeronic interaction rises with $Y$, reaching values 2 and 1.5 at $Y = 6$ for variants I and II respectively. However this difference is far larger for the eikonal functions, shown in Figs. 10 and 11 at $b = 0$. The eikonal function for a single BFKL exchange rises up to values of the order $10^9$ at $Y = 6$, whereas with pomeronic interactions we find values around 100 or 1000 for variants I and II. It is remarkable that, with the pomeronic interaction switched on, the eikonal function actually diminishes with $y$ for central collisions. Therefore the rise of the cross-section is totally due to peripheral collisions, where, with a low nuclear density, the non-linear effects

are small and the fields grow according to the pure linear BFKL equation.

## 5 Discussion

We have made the first attempt to solve the equations which describe nucleus–nucleus scattering in the framework of the perturbative QCD with a large number of colors and a fixed coupling constant. The natural iterative approach has been found to converge in a restricted domain of not too high scaled rapidities and atomic number of participants. Physical rapidities covered by the convergence range depend on the value of the coupling constant. For $\alpha_s = 0.2$ they are not greater than 10 for O–O collisions and not greater than 9 for Pb–Pb collisions. The solutions in this range of $Y$ have been found to generate the gluon density which falls with $y$ (towards the central rapidity region) and somewhat spreads into the infrared region of transverse momenta, its maximum staying around $1\,\mathrm{GeV}/c$. It radically differs from the density of the isolated nucleus, which is known to steadily shift towards higher momenta, the height of its peak being practically independent of $y$. Both the eikonal function and the total cross-section are found to be damped as compared to the single pomeron exchange (by an order of magnitude for the eikonal function). The latter has been found to actually fall with energy for central collisions. However, the total cross-sections rise with energy due to peripheral collisions where non-linear effects are naturally small.

Unfortunately we have not been able to find the solutions outside the mentioned restricted domain of rapidities and atomic numbers. We do not know what sort of singularity occurs at the boundaries of this domain and even if the solutions of our equations exist at all. It is possible that a sort of phase transition occurs at these boundaries, so that the equations have to be changed.

Just to see some qualitative features of a possible solution at high rapidities and atomic numbers, we applied a simple variational procedure, approximating the fields by certain simple trial functions with a single parameter to be determined from the stationary point equation. It is hopeless to expect to study the gluon distribution from such a simple approach. One expects more reasonable answers for the eikonal and especially for the total cross-sections which are weakly dependent on moderate variations of the fields. Our results seem to indicate that with the further rise of energy the cross-sections continue to grow slowly, much slower than with a single BFKL exchange. The eikonal function in the center continues to fall, very slowly in variant II for the initial function and rather fast for variant I.

The main lesson to be learned from these first calculations is that the dynamics of nucleus–nucleus collisions is much more complicated than for collisions of a small probe on a single nucleus. The gluon densities we have found have a much more complicated form than in the latter case when they scale with the saturation momentum which grows with energy as a power. No scaling of this sort has been observed. The remaining problem is to understand the reason of the breakdown of the iterative solution at a certain value of energy and/or atomic number and to try to move beyond this value.

*Acknowledgements.* The author is most thankful to B. Vlahovic for his constant interest in this work and discussions. He is also thankful to the North Carolina Central University, USA, for financial support.

## References

1. M.A. Braun, Phys. Lett. B **483**, 115 (2000)
2. I.I. Balitsky, Nucl. Phys. B **463**, 99 (1996)
3. Yu.V. Kovchegov, Phys. Rev. D **60**, 034008 (1999); D **61**, 074018 (2000)
4. M.A. Braun, Eur. Phys. J C **16**, 337 (2000)
5. E.M. Levin, K. Tuchin, Nucl. Phys. B **573**, 833 (2000); A **693**, 787 (2001); E.M. Levin, M. Lublinsky, Nucl. Phys. A **696**, 833 (2001)
6. N. Armesto, M.A. Braun, Eur. Phys. J. C **20**, 517 (2001); C **22**, 351 (2001)
7. A.S. Pak, A.V. Tarasov, V.V. Uzhinsky, Ch.Tseren, Yad. Fiz. **30**, 102 (1979)
8. L.N. Lipatov, in Perturbative QCD, edited by A.H. Mueller, (World Scientific, Singapore 1989), p. 411
9. K. Golec-Biernat, M. Wuesthoff, Phys. Rev. D **59**, 014017 (1999); D **60**, 114023 (1999)
10. M.A. Braun, Phys. Lett. B **483**, 105 (2000)